

Calculation of Reaction Rate Constants in the Canonical and Microcanonical Ensemble

Andreas Löhle and Johannes Kästner*

*Institute for Theoretical Chemistry, University of Stuttgart, Pfaffenwaldring 55, 70569
Stuttgart, Germany*

E-mail: kaestner@theochem.uni-stuttgart.de

Abstract

Canonical instanton theory is a widespread approach to describe the dynamics of chemical reactions in low temperature environments when tunneling effects become dominant. It is a semiclassical theory which requires locating classical periodic orbits on the upside-down potential energy surface, so-called instantons, and the computation of second order quantum corrections. The calculation of these corrections usually involves a matrix diagonalization. In this paper we present an alternative approach, which requires to solve only linear systems of equations involving sparse matrices. Furthermore the proposed method provides a reliable and numerically stable way to obtain stability parameters in multidimensional systems, which are of particular interest in the context of microcanonical instanton theory.

Introduction

The phenomenon of tunneling is a significant feature of almost any quantum mechanical system. In the context of chemistry the effects of quantum tunneling are particularly important when it comes to rate constants for chemical reactions that take place in cold environments, for instance in gas clouds in interstellar space, or involve the transfer of light atoms such as hydrogen.¹⁻⁷ While an exact quantum mechanical treatment would be most desirable in order to assess tunneling contributions it is usually not achievable due to the high computational effort which is required for realistic and hence more complex higher dimensional systems.⁸⁻¹¹ Over the years various methods have been suggested in order to handle these problems. A promising and nowadays widespread approach is what is usually referred to as canonical instanton theory. It is in essence a semiclassical theory which has appeared in somewhat different formulations since the 1960's.¹²⁻¹⁶ A common approach to introduce instanton theory is the imaginary- F premise which relates the free energy F of the system

to the thermal reaction rate constant k as¹⁶⁻¹⁸

$$k(\beta) = -\frac{2}{\hbar} \text{Im } F \approx \frac{2}{\hbar\beta} \frac{\text{Im } Q}{\text{Re } Q} \quad (1)$$

whereby Q is the system's canonical partition function and β is the inverse temperature, $\beta = 1/(k_B T)$. The task of calculating $k(\beta)$ is therefore reduced to finding the real and imaginary part of the partition function whereby the real part represents the partition function of the reactant state Q_{RS} and the imaginary part the partition function of the transition state Q_{TS} . By using a well known analogy between the Feynman path integral representation of the Schrödinger propagator in quantum mechanics and the calculation of the partition function in statistical physics one obtains a path integral representation in imaginary time¹⁹ for the partition function.

$$Q = \int d\mathbf{x} \langle \mathbf{x} | e^{-\beta \hat{H}} | \mathbf{x} \rangle \quad (2)$$

$$= \oint \mathcal{D}\mathbf{x}(\tau) e^{-\mathcal{S}_{\text{E}}[x(\tau)]} \quad (3)$$

with the Euclidean action functional given by

$$\mathcal{S}_{\text{E}}[x(\tau)] = \int \frac{M\dot{x}(\tau)^2}{2} + V(x(\tau)) d\tau \quad (4)$$

and a Hamiltonian of the form $\hat{H} = P^2/(2M) + V(x)$. The path integral in Eq. (3) is then approximated by the action of the classical solutions, which give the dominant contributions to the path integral, and the effect of deviations $\delta\mathbf{x}$ from the classical path. The canonical partition function, using this semiclassical approximation, can therefore be written as

$$Q^{\text{SC}} = \sum_i F_i e^{-S_{\text{cl}}^i} \quad (5)$$

where $\mathcal{S}_{\text{cl}}^i$ is the Euclidean action of the i^{th} classical solution and F_i is the fluctuation factor that contains quantum corrections up to second order. The classical trajectories are solutions to the classical equation of motion in imaginary time $m\ddot{\mathbf{x}} = \nabla V$. The sign change of the potential is a consequence of the Wick rotation from real to imaginary time. Usually two classical solutions can be found. One is a particle resting still at $\mathbf{x}(\tau) = \mathbf{x}_{\text{RS}}$ corresponding to Q_{RS} , the fluctuation factor F_{RS} of which is entirely real. A second solution, the so-called instanton, is an unstable periodic orbit with the period $\beta\hbar$ and an entirely imaginary fluctuation factor F_{Inst} . The rate constant is then given by

$$k(\beta) = \frac{2}{\hbar\beta} \frac{F_{\text{Inst}}}{F_{\text{RS}}} e^{-(\mathcal{S}_{\text{Inst}} - \mathcal{S}_{\text{RS}})/\hbar}. \quad (6)$$

To locate an instanton, the path is discretized into P points (images or replicas of the system) and stationary points of the discretized Euclidean action functional are searched for, rather than integrating the classical equation of motion with the right initial conditions. For a system with D spatial degrees of freedom the action functional becomes a function of DP variables. The instanton search can nowadays efficiently be done by using a truncated Newton search.^{20–23} For the fluctuation factor this discretization scheme yields a multidimensional Gaussian integral of the form

$$F = \int_{-\infty}^{\infty} \exp\left(-\frac{1}{2} \sum_{i,j=1}^{DP} A_{ij} x_i x_j\right) d^{DP} x = \sqrt{\frac{(2\pi)^{DP}}{\det \mathbf{A}}} \quad (7)$$

where \mathbf{A} is $PD \times PD$ matrix which contains the Hessians of the potential along all P discrete points of the instanton trajectory.²³ The final result on the right hand side of Eq. (7) is only applicable if \mathbf{A} is positive definite. In the case of the instanton, which is a saddle point of the discretized action functional, this is not the case as it has one negative eigenvalue and at least one zero eigenvalue. However, there exist ways to deal with these eigenvalues in a physically sensible manner and render F finite.^{24,25} The conventional way of obtaining F is therefore to obtain the full eigenvalue spectrum of \mathbf{A} .^{11,18,20–23,26–32} We will refer to this method from now

on as the determinant method. Since diagonalizing a matrix is one of the most demanding tasks in terms of the computational effort required, a faster approach is desirable. In this paper we are going to present a method that allows a much faster calculation of F .

Rather than using the straightforward way of calculating the discretized path integral for the canonical partition function by solving a product of Gaussian integrals, we start in the microcanonical ensemble and, via a steepest descent approximation, obtain an expression for the fluctuation factor. The approach bears some similarities to previous work,^{33–35} however it avoids the construction of a coordinate system which separates reactive and orthogonal modes along the instanton path. It only requires solving two linear systems of equations.

The paper is organized as follows. First we briefly review the basics of microcanonical instanton theory as well as the definitions of the monodromy matrix and the Van-Fleck propagator. Then we present the necessary algorithms to compute the quantities previously derived in order to compute F . Finally we test the new methods on two different systems, the analytic Müller–Brown potential and a chemical reaction with $V(x)$ and its derivatives calculated on-the-fly by density functional theory. In all cases the results are compared to the conventional determinant method. Finally we discuss the advantages and disadvantages of the new method.

Theory

Microcanonical Instanton Theory

The key quantity of microcanonical instanton theory is the so called cumulative reaction probability $P(E)$,¹⁴ which is the result of averaging all state-to-state cross sections for a system at a fixed energy E . The microcanonical rate constant $k(E)$ can then be calculated as follows³⁶

$$k(E) = \frac{1}{2\pi\hbar} \frac{P(E)}{\Gamma_r(E)} \tag{8}$$

with $\Gamma_r(E)$ being the density of states of the reactant. An efficient way to obtain $P(E)$ directly is the use of the quantum flux-flux autocorrelation formalism^{37,38} which gives an exact expression for $P(E)$

$$P(E) = 2\pi^2\hbar^2\text{tr}\left(\delta(E - \hat{H})\hat{F}\delta(E - \hat{H})\hat{F}\right) \quad (9)$$

where $\delta(E - \hat{H})$ is the density operator in the microcanonical ensemble and \hat{F} is the quantum mechanical analogue of the classical flux function which counts the number of elementary reactions from reactant to product and is given by

$$\hat{F} = \frac{i}{\hbar} [\hat{H}, \hat{\theta}(s)]. \quad (10)$$

Here, $\hat{\theta}$ is the Heaviside step function and s denotes a parameter that is negative on the reactant side of a dividing surface and positive on the product side. In one dimension, $P(E)$ can be obtained by a variety of methods, including a direct numerical solution of Schrödinger's equation. Instanton theory provides a semiclassical approximation for $P(E)$ for a system with D_ν vibrational degrees of freedom as:¹⁴

$$P_{\text{SC}}(E) = \sum_{k=1}^{\infty} (-1)^{k-1} \prod_{i=1}^{D_\nu-1} \frac{1}{2 \sinh(ku_i(E)/2)} \times \exp(-k\mathcal{S}_0(E)) \quad (11)$$

$$= \sum_{k=1}^{\infty} (-1)^{k-1} F_{k,\perp}(E) \exp(-k\mathcal{S}_0(E)). \quad (12)$$

Here and in the following, atomic units ($\hbar = e = m_e = 4\pi\epsilon_0 = 1$) and mass weighted coordinates are used, $\mathcal{S}_0 = \int \dot{\mathbf{x}}^2/2d\tau$ is the shortened action, and $u_i(E)$ are the stability parameters of the instanton path. The corresponding thermal rate constant can be obtained by thermally averaging $k(E)$ which results in a Laplace transform of $P(E)$. If we use Eq. (12) as approximation for $P(E)$ we assume the rotational motion to be separable from the internal motion. Eq. (12) is essentially $P(E, J)$ for $J = 0$. In the J -shifting approximation^{39,40} the

rotational dependence is taken out of the integral such that the thermal rate constant is given by

$$k(\beta) = \frac{Q_{\text{t-r}}}{2\pi Q_{\text{RS}}} \int_{-\infty}^{\infty} P_{\text{SC}}(E) \exp(-\beta E) dE \quad (13)$$

where $Q_{\text{t-r}}$ is the ratio of translational and rotational partition functions of transition state and reactant. Rotational partition functions are typically estimated from rigid rotors.

In principle one has to sum over all classical solutions with the same energy E , which also includes solutions that pass the instanton's orbit multiple times. Since the contributions of those trajectories are weighted with $\exp(-k\mathcal{S}_0)$, with k being the multiplicity of the orbit, their contributions decay exponentially and can be neglected. However, for an instanton with an energy E close to the transition state's energy E_{TS} this becomes an increasingly bad approximation since close to E_{TS} the shortened action \mathcal{S}_0 gets smaller and ultimately vanishes at $E = E_{\text{TS}}$. This neglect of contributions from repetitions of the instanton orbit leads to the familiar overestimation of $k(\beta)$ close to the crossover temperature T_c . Techniques to correct for that were proposed.^{41,42} In order to perform the Laplace transform in Eq. (13) we approximate the integral for $k = 1$ via a steepest descent approach such that

$$\int_{-\infty}^{\infty} F_{\perp}(E) e^{-(\beta E + \mathcal{S}_0)} dE \approx \sqrt{\frac{2\pi}{\frac{d^2 \mathcal{S}_0}{dE^2}}} F_{\perp}(E_0) e^{-(\beta E_0 + \mathcal{S}_0(E_0))} \quad (14)$$

where E_0 satisfies the condition $\frac{d}{dE}(\mathcal{S}_0 + \beta E) = 0$. From that we obtain $\frac{d\mathcal{S}_0}{dE} = -\beta$ which results in¹⁴

$$k(\beta) = \frac{Q_{\text{t-r}}}{\sqrt{2\pi} Q_{\text{RS}}} \sqrt{-\frac{dE}{d\beta}} \prod_{i=1}^{D_{\nu}-1} \frac{1}{2 \sinh(u_i(E_0)/2)} e^{-\mathcal{S}_{\text{Inst}}} \quad (15)$$

with $\mathcal{S}_{\text{Inst}} = \mathcal{S}_{\text{E}}(E_0)$. So once an instanton is located $\frac{dE}{d\beta}$ and the stability parameters u_i have to be determined in order to calculate the rate constant.

The Van-Fleck Propagator and the Monodromy Matrix

To determine the stability parameters we have to find a way to compute the monodromy matrix⁴³ first. For that purpose we will need to evaluate the Van-Fleck propagator which is a semiclassical expression for the Schrödinger propagator. In imaginary time it is given by^{44,45}

$$K_{\text{sc}}(\mathbf{x}'', \mathbf{x}', it) = \left(\frac{1}{2\pi}\right)^{\frac{D}{2}} \sqrt{\left| \text{Det} \left(-\frac{\partial^2 \mathcal{S}_E}{\partial x'_i \partial x''_j} \right) \right|} e^{-\mathcal{S}_E + i\Phi} \quad (16)$$

whereby Φ is

$$\Phi = -\frac{\pi}{2}\nu \quad (17)$$

and ν is called the Maslov–Morse index which counts the number of zeros of the determinant. Eq. (16) gives the semiclassical probability amplitude of a particle with unit mass moving from \mathbf{x}' to \mathbf{x}'' in imaginary time $\tau = it$. To calculate the partition function we have to take the trace of Eq. (16)

$$Q^{\text{SC}} = \int K_{\text{sc}}(\mathbf{x}, \mathbf{x}, \beta) d\mathbf{x} \quad (18)$$

In order to evaluate the trace we perform a steepest descent integration. Using that for the classical solution $\frac{\partial \mathcal{S}_E}{\partial \mathbf{x}} = 0$ and

$$\frac{\partial^2 \mathcal{S}_E}{\partial \mathbf{x}^2} = \left(\frac{\partial^2 \mathcal{S}_E}{\partial \mathbf{x}' \mathbf{x}'} + 2 \frac{\partial^2 \mathcal{S}_E}{\partial \mathbf{x}' \mathbf{x}''} + \frac{\partial^2 \mathcal{S}_E}{\partial \mathbf{x}'' \mathbf{x}''} \right) \Big|_{\mathbf{x}' = \mathbf{x}'' = \mathbf{x}} \quad (19)$$

we finally get

$$Q^{\text{SC}} = \sum_i Q^{\text{SC},i} \quad (20)$$

with

$$\begin{aligned}
Q^{\text{SC},i} &= \sqrt{\frac{\left| -\frac{\partial^2 \mathcal{S}_{\text{E}}^i}{\partial \mathbf{x}' \partial \mathbf{x}''} \right|_{x'=x''=x}}{\left| \frac{\partial^2 \mathcal{S}_{\text{E}}^i}{\partial \mathbf{x}' \partial \mathbf{x}'} + 2 \frac{\partial^2 \mathcal{S}_{\text{E}}^i}{\partial \mathbf{x}' \partial \mathbf{x}''} + \frac{\partial^2 \mathcal{S}_{\text{E}}^i}{\partial \mathbf{x}'' \partial \mathbf{x}''} \right|_{x'=x''=x}}} \times \\
&\exp\left(-\mathcal{S}_{\text{cl}}^i - i\frac{\pi}{2}\nu_i\right) \\
&= F_i \exp\left(-\mathcal{S}_{\text{cl}}^i\right) \exp\left(-i\frac{\pi}{2}\nu_i\right)
\end{aligned} \tag{21}$$

Since the classical solution that corresponds to the reactant state is simply a particle resting still, it has no turning points, hence $\nu = 0$ and the Euclidean action simply becomes $\mathcal{S}_{\text{RS}} = \beta V(\mathbf{x}_{\text{RS}})$. The instanton is a closed orbit and therefore ν depends on how often the particle reaches the turning points. In this case ν can have values of $2k$ where k gives the number of repetitions of the instanton orbit. However, we have to add an additional phase factor of $-i\pi/2$ in order to account for the fact that the instanton travels only in the classically forbidden region and therefore only contributes to the imaginary part of the partition function. If we consider one orbit only for the instanton we get $\nu = 2$ and the fluctuation factor turns imaginary as $\exp(-i(\nu\frac{\pi}{2} + \frac{\pi}{2})) = i$. This gives for the partition functions of the reactant and the transition states

$$Q_{\text{RS}} = F_{\text{RS}} e^{-\mathcal{S}_{\text{RS}}} \tag{22}$$

$$Q_{\text{Inst}} = iF_{\text{Inst}} e^{-\mathcal{S}_{\text{Inst}}}. \tag{23}$$

The term F can in principle be divergent. This is due to symmetries present in the system which lead to an over-counting of real physical states and therefore to a diverging partition function. Since the instanton is a closed orbit the action is invariant with respect to the choice of the starting and end point as $\mathbf{x}' = \mathbf{x}'' = \mathbf{x}$. Furthermore rotation and translational invariance are also symmetries that lead to diverging terms, yet these can easily be handled as those symmetries are also present in the reactant partition function and therefore cancel

one another if one is only interested in their ratios. In order to handle the divergent terms we express F in a different representation. We construct a matrix \mathbf{M} with the following entries

$$\mathbf{M} = \begin{pmatrix} -\mathbf{b}^{-1}\mathbf{a} & -\mathbf{b}^{-1} \\ \mathbf{b} - \mathbf{c}\mathbf{b}^{-1}\mathbf{a} & -\mathbf{c}\mathbf{b}^{-1} \end{pmatrix} \quad (24)$$

whereby \mathbf{a} , \mathbf{b} and \mathbf{c} are defined as

$$\mathbf{a} = \left. \frac{\partial \mathcal{S}_E}{\partial \mathbf{x}' \partial \mathbf{x}'} \right|_{\mathbf{x}' = \mathbf{x}'' = \mathbf{x}} \quad (25)$$

$$\mathbf{b} = \left. \frac{\partial \mathcal{S}_E}{\partial \mathbf{x}' \partial \mathbf{x}''} \right|_{\mathbf{x}' = \mathbf{x}'' = \mathbf{x}} \quad (26)$$

$$\mathbf{c} = \left. \frac{\partial \mathcal{S}_E}{\partial \mathbf{x}'' \partial \mathbf{x}''} \right|_{\mathbf{x}' = \mathbf{x}'' = \mathbf{x}} \quad (27)$$

such that the fluctuation factor in Eq. (21) can be written as

$$F = \sqrt{\frac{|\mathbf{b}|}{|\mathbf{a} + 2\mathbf{b} + \mathbf{c}|}} = \sqrt{\frac{(-1)^D}{|\mathbf{M} - \mathbf{1}|}}. \quad (28)$$

If \mathbf{M} is represented in its eigenbasis one can immediately see that the right-hand side of Eq. (28) diverges as \mathbf{M} has eigenvalues of $\lambda = 1$. These correspond to the symmetries of the system. Furthermore \mathbf{M} is a symplectic matrix meaning that eigenvalues always appear in pairs. If λ_i is an eigenvalue so is $1/\lambda_i$. The matrix \mathbf{M} is called the monodromy matrix.⁴³ It contains information about how significantly a solution to the classical equations of motion deviates from its reference position and momentum under an infinitesimal perturbation of $\delta \mathbf{x}_0$ and $\delta \mathbf{p}_0$ after one period T_0 has passed.

$$\begin{pmatrix} \delta \mathbf{x} \\ \delta \mathbf{p} \end{pmatrix} = \mathbf{M}(T_0) \begin{pmatrix} \delta \mathbf{x}_0 \\ \delta \mathbf{p}_0 \end{pmatrix} \quad (29)$$

where \mathbf{M} is the solution to the linearized equations of motion

$$\frac{d}{dt}\mathbf{M}(t) = \begin{pmatrix} 0 & \mathbf{1} \\ -\mathbf{V}''(\mathbf{x}(t)) & 0 \end{pmatrix} \mathbf{M}(t) \quad (30)$$

evaluated at $t = T_0$. Thus, the eigenvalues of \mathbf{M} inform about the stability of the trajectory. Real values of λ are connected to unstable modes. With the definition $\lambda_i = e^{u_i}$ we get the fluctuation factor

$$F = \sqrt{\prod_{i=1}^D \frac{-1}{(e^{u_i} - 1) \cdot (e^{-u_i} - 1)}} \quad (31)$$

$$= \sqrt{\prod_{i=1}^D \frac{-1}{2 - 2 \cosh(u_i)}} \quad (32)$$

$$= \prod_{i=1}^D \frac{1}{2 \sinh(u_i/2)}. \quad (33)$$

The fluctuation factor F including all D degrees of freedom is obviously divergent as it has at least one, in the case of rotational and translational symmetries an additional six, zero-valued stability parameters $u_i = 0$. As mentioned before we can simply ignore the translational and rotational ones as the fluctuation factor only covers vibrations. Using Eq. (6), gives for the rate constant

$$k(\beta) = \frac{2}{\beta} Q_{\text{t-r}} \frac{2 \prod_{j=1}^{D_\nu} \sinh(u_j^{\text{RS}}/2)}{\prod_{i=1}^{D_\nu-1} \sinh(u_i^{\text{Inst}}/2)} F_{\parallel}^{\text{Inst}} e^{-\mathcal{S}_{\text{Inst}} + \mathcal{S}_{\text{RS}}}. \quad (34)$$

The parallel fluctuation factor $F_{\parallel}^{\text{Inst}}$, which only appears in the instanton partition function, can not be described by Eq. (33) due to u_i being zero. However, it can be addressed by applying the Faddeev–Popov trick to avoid the over-counting of ghost states in order to render the partition function finite.²⁴ In this case, however, we can simply compare Eq. (6)

with Eq. (15), using $F^{\text{Inst}} = F_{\perp}^{\text{Inst}} F_{\parallel}^{\text{Inst}}$, and obtain

$$\begin{aligned} \frac{2}{\beta} \frac{Q_{\text{t-r}} Q_{\text{Inst}}}{Q_{\text{RS}}} &= \frac{Q_{\text{t-r}}}{\sqrt{2\pi} Q_{\text{RS}}} \sqrt{-\frac{dE}{d\beta}} F_{\perp}^{\text{Inst}} e^{-\mathcal{S}_{\text{Inst}}} \\ \frac{2}{\beta} F^{\text{Inst}} e^{-\mathcal{S}_{\text{Inst}}} &= \frac{1}{\sqrt{2\pi}} \sqrt{-\frac{dE}{d\beta}} F_{\perp}^{\text{Inst}} e^{-\mathcal{S}_{\text{Inst}}} \\ F_{\parallel}^{\text{Inst}} &= \sqrt{\frac{\beta^2}{8\pi}} \sqrt{-\frac{dE}{d\beta}}. \end{aligned} \quad (35)$$

Using the result of Eq. (35) we obtain the final rate constant expression

$$k(\beta) = \frac{Q_{\text{t-r}}}{\sqrt{2\pi}} \sqrt{-\frac{dE}{d\beta}} \frac{2 \prod_{j=1}^{D_{\nu}} \sinh(u_j^{\text{RS}}/2)}{\prod_{i=1}^{D_{\nu}-1} \sinh(u_i^{\text{Inst}}/2)} e^{-\mathcal{S}_{\text{Inst}} + \mathcal{S}_{\text{RS}}}. \quad (36)$$

Overall, in order to evaluate the thermal rate constant we find an instanton at given β and calculate its stability parameters u_i , as well as $\frac{dE}{d\beta}$. In a previous paper⁴² we have presented several methods using different approximative schemes to calculate u_i as an alternative to the traditional way of integrating the linearized equations of motions, Eq. (30). Here, we present a different approach making use of Eq. (24), which allows us to calculate the monodromy matrix by using the second variations of \mathcal{S}_{E} . It is exact in the limit of $P \rightarrow \infty$ but appears to be numerically more stable than integrating Eq. (30). In case of the reactant state, $u_i^{\text{RS}} \equiv \omega_i^{\text{RS}} \beta$ with ω_i^{RS} being the reactant's vibrational frequencies, see Appendix. However, in order to benefit from error cancellation at finite P , we use the same numerical algorithm for the reactant state as we do for the instanton. In the following, we present a numerical algorithm to evaluate $\frac{dE}{d\beta}$ and u_i .

Numerical implementation

In the following sections we present two algorithms in order to calculate the necessary quantities mentioned in the previous sections. In both cases we rely on a discretization of the classical equation of motion in imaginary time, i.e. in the upside-down potential $-V$, which

yields

$$\ddot{\mathbf{x}}(\tau) = \nabla V \quad (37)$$

$$(-2\mathbf{x}_i + \mathbf{x}_{i+1} + \mathbf{x}_{i-1}) \frac{1}{\Delta\tau^2} = \nabla V(\mathbf{x}_i) \quad (38)$$

$$(2\mathbf{x}_i - \mathbf{x}_{i+1} - \mathbf{x}_{i-1}) + \frac{\beta^2}{P^2} \nabla V(\mathbf{x}_i) = 0. \quad (39)$$

The vector \mathbf{x}_i is a D dimensional array that contains the positions for every degree of freedom at the i^{th} image. P is the number of discrete points and β is in this context the period in imaginary time such that $\Delta\tau = \frac{\beta}{P}$.

Furthermore it is worth mentioning that the kind of instanton solutions that we use in the following have the property that each image appears exactly twice as the spatial coordinates of the trajectory from the reactant to the product side are the same as on the way back from product to reactant. This leads to $\mathbf{x}_i = \mathbf{x}_{P-i+1}$. However, the following derivation does not use this fact and the algorithms are valid for any closed trajectory which may or may not possess turning points.

Calculation of $\frac{dE}{d\beta}$

In order to calculate the change of the energy of the instanton solution with respect to β we start by looking at the energy conservation of the instanton solution.^{31,46} Since we are in imaginary time the momentum in the classically forbidden region is purely imaginary and therefore the energy E is given by

$$E = \frac{i^2 \mathbf{p}^2}{2} + V(\mathbf{x}) \quad (40)$$

$$= -\frac{\mathbf{p}^2}{2} + V(\mathbf{x}). \quad (41)$$

It is conserved along the orbit. The discretized form of Eq. (41) reads

$$E = \lim_{P \rightarrow \infty} \left(-\frac{(\mathbf{x}_i - \mathbf{x}_{i-1})^2}{2} \left(\frac{P}{\beta} \right)^2 + \frac{1}{2}(V(\mathbf{x}_i) + V(\mathbf{x}_{i-1})) \right) \quad (42)$$

Since a change in β means that a new instanton solution for a new temperature has to be found we can interpret the points \mathbf{x}_i along the trajectory to be a function of β , thus $\mathbf{x}_i = \mathbf{x}_i(\beta)$. If we now differentiate Eq. (42) with respect to β we get

$$\begin{aligned} \frac{dE}{d\beta} = \lim_{P \rightarrow \infty} & \left(\frac{P^2}{\beta^3} (\mathbf{x}_i - \mathbf{x}_{i-1})^2 \right. \\ & - \frac{P^2}{\beta^2} (\mathbf{x}_i - \mathbf{x}_{i-1}) \left(\frac{d\mathbf{x}_i}{d\beta} - \frac{d\mathbf{x}_{i-1}}{d\beta} \right) \\ & \left. + \frac{1}{2} \left(\frac{\partial V}{\partial \mathbf{x}_i} \frac{d\mathbf{x}_i}{d\beta} + \frac{\partial V}{\partial \mathbf{x}_{i-1}} \frac{d\mathbf{x}_{i-1}}{d\beta} \right) \right) \quad (43) \end{aligned}$$

In order to evaluate Eq. (43) one has to calculate $\frac{d\mathbf{x}_i}{d\beta}$. The first step is to differentiate Eq. (39) with respect to β and replacing $\frac{d\mathbf{x}_i}{d\beta}$ by \mathbf{q}_i . This yields⁴⁶

$$\left(2 + \frac{\beta^2}{P^2} \nabla^2 V(\mathbf{x}_i) \right) \mathbf{q}_i - \mathbf{q}_{i+1} - \mathbf{q}_{i-1} = -\frac{2\beta}{P^2} \nabla V(\mathbf{x}_i) \quad (44)$$

Eq. (44) is a linear system of equations of the form

$$\mathbf{A}\mathbf{q} = \mathbf{b} \quad (45)$$

or, using an index notation for images and degrees of freedom,

$$\sum_{i'=1}^P \sum_{j'=1}^D A_{i,j,i',j'} q_{i',j'} = b_{i,j}. \quad (46)$$

Here,

$$\mathbf{A} = \begin{pmatrix} \mathbf{K}_1 & -\mathbf{I} & 0 & \dots & 0 & -\mathbf{I} \\ -\mathbf{I} & \ddots & -\mathbf{I} & \ddots & \ddots & 0 \\ 0 & -\mathbf{I} & \mathbf{K}_i & \ddots & \ddots & \vdots \\ \vdots & \ddots & \ddots & \mathbf{K}_{i+1} & -\mathbf{I} & 0 \\ 0 & \ddots & \ddots & -\mathbf{I} & \ddots & -\mathbf{I} \\ -\mathbf{I} & 0 & \dots & 0 & -\mathbf{I} & \mathbf{K}_P \end{pmatrix} \quad (47)$$

where $\mathbf{K}_i = 2\mathbf{I} + \frac{\beta^2}{P^2}\mathbf{V}''(\mathbf{x}_i)$, \mathbf{I} being the $D \times D$ unit matrix and

$$\mathbf{b} = -\frac{2\beta}{P^2} \begin{pmatrix} \nabla_1 V(\mathbf{x}_1) \\ \vdots \\ \nabla_D V(\mathbf{x}_1) \\ \nabla_1 V(\mathbf{x}_2) \\ \vdots \\ \nabla_j V(\mathbf{x}_i) \\ \vdots \\ \nabla_D V(\mathbf{x}_P) \end{pmatrix}. \quad (48)$$

Solving Eq. (45) requires the knowledge of all Hessians as well as gradients along the instanton path. The matrix \mathbf{A} is a symmetric sparse ($PD \times PD$) matrix.

Having obtained $\frac{d\mathbf{x}_i}{d\beta} = \mathbf{q}_i$ we can now determine $\frac{dE}{d\beta}$ by choosing any arbitrary point \mathbf{x}_i and use it in Eq. (43). In practice the value of $\frac{dE}{d\beta}$ will slightly vary along the path due to numerical errors. Therefore, we choose one of the turning points as the distance between the current and the next point is the shortest in that case.

Calculation of $\frac{\partial \mathcal{S}_E}{\partial \mathbf{x}' \partial \mathbf{x}''}$

Since an analytical treatment of the second derivatives of \mathcal{S}_E is only possible in the case of a separable potential in which the orthogonal components of the potential have a linear or quadratic form, we have to find a way to determine these necessary expressions numerically, which is achieved by following previous work.^{31,46} We start with the discretized Euclidean action for an instanton that starts at $\tau = 0$ at the point $\mathbf{x}' = \mathbf{x}_0$ and ends at $\tau = \beta$ at the point $\mathbf{x}'' = \mathbf{x}_P$. Furthermore a constant time interval $\Delta\tau = \beta/P$ is used because we consider an arbitrary open path with $P + 1$ images to derive the first and second variations and only then close the path by setting $\mathbf{x}' = \mathbf{x}'' = \mathbf{x}$ resulting in P independent images. The Euclidean action is

$$\mathcal{S}_E = \sum_{i=1}^P \left[\frac{1}{2} \frac{(\mathbf{x}_i - \mathbf{x}_{i-1})^2}{\Delta\tau} + \frac{\Delta\tau}{2} (V(\mathbf{x}_i) + V(\mathbf{x}_{i-1})) \right] \quad (49)$$

The first variation of Eq. (49) results in

$$\frac{\partial \mathcal{S}_E}{\partial \mathbf{x}'} = -\frac{(\mathbf{x}_1 - \mathbf{x}_0)}{\Delta\tau} + \frac{\Delta\tau}{2} V'(\mathbf{x}_0) \quad (50)$$

$$\frac{\partial \mathcal{S}_E}{\partial \mathbf{x}''} = \frac{(\mathbf{x}_P - \mathbf{x}_{P-1})}{\Delta\tau} + \frac{\Delta\tau}{2} V'(\mathbf{x}_P) \quad (51)$$

To calculate the second variation of Eq. (49) we have to keep in mind that while \mathbf{x}' and \mathbf{x}'' stay fixed, the points in between change. In this case we regard \mathbf{x}_i for $i \in [1, \dots, P - 1]$ as a function of \mathbf{x}_0 and \mathbf{x}_P . This results in the second variation

$$\frac{\partial^2 \mathcal{S}_E}{\partial \mathbf{x}' \partial \mathbf{x}''} = -\frac{1}{\Delta\tau} \frac{\partial \mathbf{x}_1}{\partial \mathbf{x}_P} \quad (52)$$

$$\frac{\partial^2 \mathcal{S}_E}{\partial \mathbf{x}' \partial \mathbf{x}'} = \frac{1}{\Delta\tau} \left(\mathbf{I} - \frac{\partial \mathbf{x}_1}{\partial \mathbf{x}_0} \right) + \frac{\Delta\tau}{2} \mathbf{V}''(\mathbf{x}_0) \quad (53)$$

$$\frac{\partial^2 \mathcal{S}_E}{\partial \mathbf{x}'' \partial \mathbf{x}''} = \frac{1}{\Delta\tau} \left(\mathbf{I} - \frac{\partial \mathbf{x}_{P-1}}{\partial \mathbf{x}_P} \right) + \frac{\Delta\tau}{2} \mathbf{V}''(\mathbf{x}_P) \quad (54)$$

To be able to use these expressions we have to find a way to calculate the terms $\frac{\partial \mathbf{x}_{P-1}}{\partial \mathbf{x}_P}$ and $\frac{\partial \mathbf{x}_2}{\partial \mathbf{x}_1}$. This can be done in the same way as before based on Eq. (39). We differentiate Eq. (39) with respect to \mathbf{x}_α where α can be either 0 or P and get⁴⁶

$$2 \frac{\partial \mathbf{x}_i}{\partial \mathbf{x}_\alpha} - \frac{\partial \mathbf{x}_{i+1}}{\partial \mathbf{x}_\alpha} - \frac{\partial \mathbf{x}_{i-1}}{\partial \mathbf{x}_\alpha} + \Delta \tau^2 \mathbf{V}''(\mathbf{x}_i) \frac{\partial \mathbf{x}_i}{\partial \mathbf{x}_\alpha} = 0 \quad (55)$$

$$\left(2\mathbf{I} + \Delta \tau^2 \mathbf{V}''(\mathbf{x}_i)\right) \mathbf{J}_i - \mathbf{J}_{i+1} - \mathbf{J}_{i-1} = 0 \quad (56)$$

$$\mathbf{K}_i \mathbf{J}_i - \mathbf{J}_{i+1} - \mathbf{J}_{i-1} = 0 \quad (57)$$

where $i \in [1, \dots, P-1]$ and $\mathbf{J}_i \equiv \frac{\partial \mathbf{x}_i}{\partial \mathbf{x}_\alpha}$ is a $D \times D$ matrix with the following boundary conditions for $\alpha = 1$

$$\mathbf{J}_{i=0}^{\alpha=0} = \mathbf{I} \quad (58)$$

$$\mathbf{J}_{i=P}^{\alpha=0} = 0 \quad (59)$$

and for $\alpha = P$

$$\mathbf{J}_{i=0}^{\alpha=P} = 0 \quad (60)$$

$$\mathbf{J}_{i=P}^{\alpha=P} = \mathbf{I} \quad (61)$$

In principle what we have obtained here is another representation of Eq. (30). If we take Eq. (55), which is a second order differential equation of the form $\ddot{\mathbf{J}}(\tau) = -\mathbf{V}''(\mathbf{x}(\tau))\mathbf{J}(\tau)$, and transform it to first order we get the familiar matrix differential equation of Eq. (30). As solving Eq. (30) with a Runge–Kutta approach turned out rather unstable in practice⁴² for low values of P we will instead focus on solving Eq. (55). First we transform Eq. (55) to a linear system of equations of the form

$$\mathbf{C}\mathbf{q} = \mathbf{d} \quad (62)$$

in which \mathbf{C} is matrix of dimension $D^2(P-1) \times D^2(P-1)$, which is given as

$$\mathbf{C} = \begin{pmatrix} \mathbf{G}_1 & -\mathbf{I} & 0 & \cdots & \cdots & 0 \\ -\mathbf{I} & \ddots & -\mathbf{I} & \ddots & \cdots & 0 \\ 0 & -\mathbf{I} & \mathbf{G}_i & \ddots & \ddots & \vdots \\ \vdots & \ddots & \ddots & \mathbf{G}_{i+1} & \ddots & \vdots \\ \vdots & \ddots & \ddots & \ddots & \ddots & -\mathbf{I} \\ 0 & 0 & \cdots & \cdots & -\mathbf{I} & \mathbf{G}_{P-1} \end{pmatrix} \quad (63)$$

with \mathbf{I} being a $D^2 \times D^2$ -dimensional unit matrix and \mathbf{G}_i is a $D^2 \times D^2$ matrix of the form

$$\mathbf{G}_i = \begin{pmatrix} \mathbf{K}_i & 0 \\ & \ddots \\ 0 & \mathbf{K}_i \end{pmatrix}. \quad (64)$$

The right hand side of Eq. (62) is given by the column vectors of \mathbf{J}_0 or \mathbf{J}_P depending on whether we want to calculate $\frac{\partial}{\partial \mathbf{x}_P}$ or $\frac{\partial}{\partial \mathbf{x}_0}$. For example in the case of a system with $D = 2$,

\mathbf{d} is given by

$$d = \begin{pmatrix} 1 \\ 0 \\ 0 \\ 1 \\ 0 \\ \vdots \\ 0 \end{pmatrix} \text{ for } \frac{\partial}{\partial \mathbf{x}_0}, d = \begin{pmatrix} 0 \\ \vdots \\ 0 \\ 1 \\ 0 \\ 0 \\ 1 \end{pmatrix} \text{ for } \frac{\partial}{\partial \mathbf{x}_P}. \quad (65)$$

Correspondingly the solutions we are looking for are given by

$$\frac{\partial \mathbf{x}_1}{\partial \mathbf{x}_0} = \begin{pmatrix} q_1 & q_3 \\ q_2 & q_4 \end{pmatrix} \quad \frac{\partial \mathbf{x}_{P-1}}{\partial \mathbf{x}_P} = \begin{pmatrix} q_{DP-4} & q_{DP-2} \\ q_{DP-3} & q_{DP-1} \end{pmatrix}. \quad (66)$$

This scheme works in general for any path whether it is open or closed. In the closed case one just sets $\mathbf{x}_0 = \mathbf{x}_P$ in Eqs. (52), (53), and (54). Instead of calculating the determinant of a $(DP \times DP)$ matrix one now has to solve a linear system of equations of the form $\mathbf{C}\mathbf{q} = \mathbf{d}$, where \mathbf{C} is a banded matrix of the size $D^2(P - 1)$.

In summary we have to evaluate Eq. (36) in order to compute the thermal rate constant $k(\beta)$. The vibrational partition function of the reactant and the orthogonal contributions to the transition state's partition function Q_{Inst} are calculated via the stability parameters, which are obtained from the eigenvalues of the monodromy matrix \mathbf{M} obtained by Eq. (24). The entries of \mathbf{M} are calculated by Eqs. (52) to (54), which require solving the linear system of equations in Eq. (62). For that, the Hessians ($\mathbf{V}''(\mathbf{x}_i)$) of all images along the path have to be known. The derivative $dE/d\beta$ is calculated by solving Eq. (45) and using the solution in Eq. (43).

The computational requirements of this algorithm are different from the determinant method. In the latter, one sparse but full matrix of size DP needs to be diagonalized, which requires $\mathcal{O}(P^3D^3)$ operations. In our algorithm, the calculation of $dE/d\beta$, i.e. solving Eq. (45), requires to solve a sparse linear system of DP equations, which again requires $\mathcal{O}(P^3D^3)$ operations. The pre-factor is 1–2 orders of magnitude lower, however. Thus, the calculations are faster by that factor. To obtain the u_i -values, a system of equations of the size $D^2(P - 1)$ has to be solved, Eq. (62). The matrix is a banded matrix with a width of only $\mathcal{O}(D^2)$, thus requiring $\mathcal{O}(PD^6)$ operations. Consequently, our algorithm is faster than the determinant method in practice, especially for small systems with many images, which is typically the case for fitted potential energy surfaces.

Applications

We applied the new method to two examples: the analytic, two-dimensional Müller–Brown potential and a rearrangement of methylhydroxycarbene to acetaldehyde with energies, gradients and Hessians calculated on-the-fly by DFT.

Müller–Brown Potential

In the Müller–Brown potential⁴⁷ we study the transition from the intermediate minimum at the coordinates $(-0.05001, 0.46669)$ over the barrier with the saddle point at $(-0.822001, 0.624314)$ to the global minimum. Since this is a two-dimensional system without rotational and translational invariance, one stability parameter is zero and another one represents the fluctuations orthogonal to the instanton path. For a particle of the mass of a hydrogen atom moving in the Müller–Brown potential, the crossover temperature is 2207 K. Figs. 1, 2 and 3 show the results for the non zero stability parameter u , the quantity $\frac{dE}{d\beta}$ and consequently the thermal rate constant $k(\beta)$, which can directly be calculated from these quantities using Eq. (36).

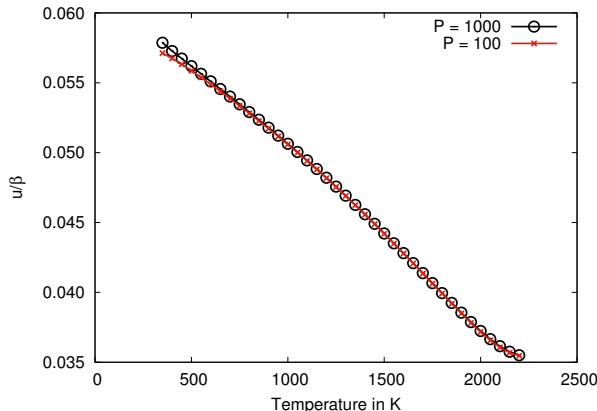


Figure 1: Stability parameter of the instanton’s orthogonal modes in the Müller–Brown potential calculated at different temperatures for different numbers of images P .

Fig. 1 demonstrates that the value of the stability parameter is rather independent of the number of images. Only at rather low temperature compared to T_c , where the rate constant is already pretty independent of the temperature are more images required to achieve a

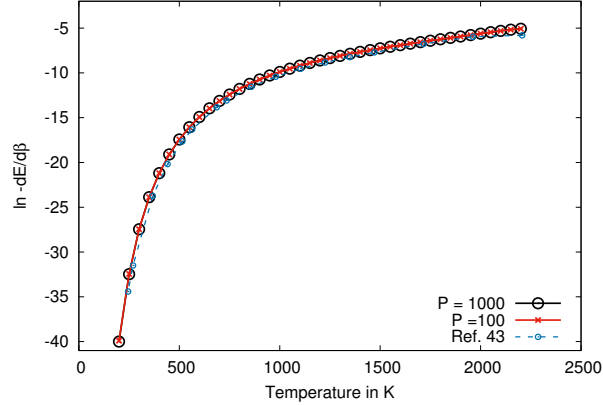


Figure 2: Change of the instanton's tunneling energy with respect to β in the Müller–Brown potential calculated at different temperatures for a different number of images P . The value of $\frac{dE}{d\beta}$ is negative for all $T < T_c$. The dashed blue line uses the approximation scheme previously proposed in Ref. 48.

converged result for u . The largest deviation occurs at the lowest temperature, $T = 350$ K, with a deviation of only 1.3% between $P = 100$ and $P = 1000$. Fig. 2 compares the result of the calculation for $\frac{dE}{d\beta}$ using the solution of Eq. (45) to an approximation scheme previously proposed in Ref. 48. They all agree very well.

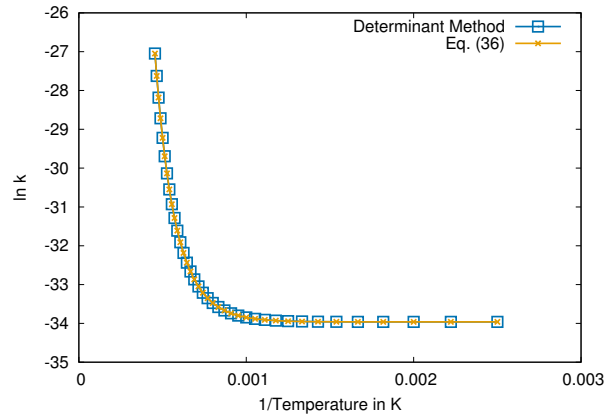


Figure 3: Rate constant in atomic units for the Müller–Brown potential. The orange line was calculated using Eq. (36) and the quantities determined in Fig. 1 and Fig. 2. The blue line was calculated with the conventional determinant method.

If we compare the results for $k(T)$ in Fig. 3 calculated with the conventional determinant method (blue) and the new approach (orange), both with 1000 images, we get to almost identical results. The largest deviation between the two methods was 0.06% at $T = 450$ K

long after the instanton converges to the final rate constant.

DFT Calculations for the Methylhydroxycarbene

The tunneling-decay of methylhydroxycarbene to acetaldehyde was previously studied experimentally and computationally.^{49,50} Here, we use this reaction to investigate the stability of our new method with respect to numerical noise in the gradients and Hessians and to provide data for a system with translational and rotational invariance. We obtained energies and their derivatives on-the-fly using DFT calculations with the B3LYP hybrid functional⁵¹⁻⁵⁶ in combination with the def2-SVP basis set.⁵⁷ These calculations were done using Turbomole v 7.0.1.⁵⁸ For the geometry optimizations and subsequent instanton calculations DL-FIND⁵⁹ was used via ChemShell⁶⁰ as interface to Turbomole. Note that here we compare methods rather than aiming at high accuracy in comparison to experiment. Nevertheless, B3LYP (with a different basis set, though) was found to reproduce more accurate calculations quite well.⁵⁰

In the calculations $P = 128$ images were used for the discretization of the instanton path unless notes otherwise. Instantons have been optimized such that the largest component of the gradient is smaller than 10^{-9} atomic units. The SCF cycles were iterated up to the change was less than 10^{-9} Hartree per iteration. The $m5$ grid⁶¹ was used.

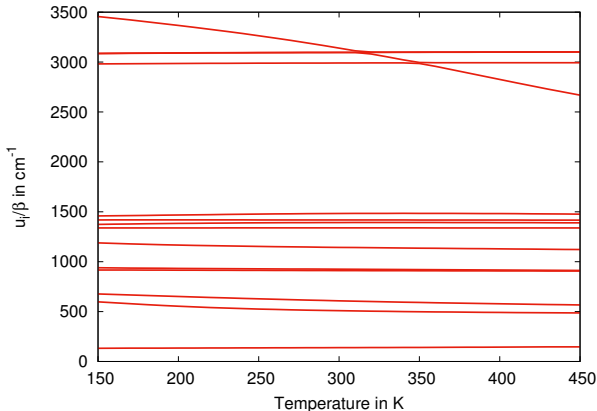


Figure 4: The 14 non-zero stability parameters for the carbene system using 128 images.

After optimizing the instanton geometries at a series of temperatures below the crossover temperature of 453 K, we calculated the stability parameters u_i using Eq. (62). For this 7-atom system there are 14 non-zero stability parameters. They can be interpreted as frequencies via $\omega_i = u_i/\beta$ as discussed previously.⁴² These stability parameters are depicted in Fig. 4. Most of them are almost independent of T . The stability parameter with the strongest T -dependence corresponds to the movement of the transferred H-atom perpendicular to the instanton path. At high temperature, the instanton path is short and in direct vicinity of the saddle point. Correspondingly, the value of the T -dependent stability parameter is close to 2660.7 cm^{-1} , the wave number of the C–H and O–H stretching mode of the transferred H. At lower T its value increases, tending towards the value of 3736.0 cm^{-1} , which corresponds to the O–H stretching mode in the reactant, methylhydroxycarbene.

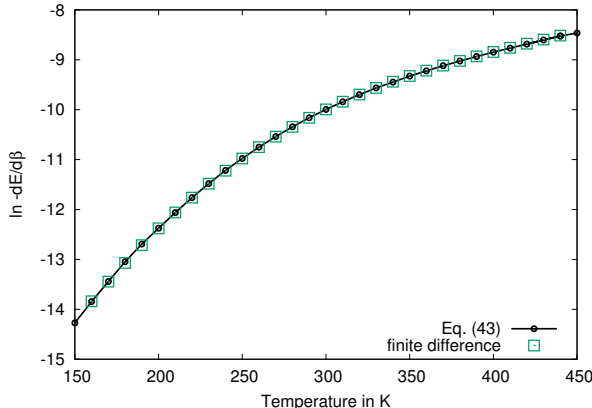


Figure 5: Change of the instanton’s tunneling energy with respect to β in for the reaction of methylhydroxycarbene to acetaldehyde calculated with 128 images. The value of $\frac{dE}{d\beta}$ is negative for all $T < T_c$. The green squares correspond to finite differences between E obtained for instantons at adjacent temperatures.

The temperature-dependence of $dE/d\beta$ is shown in Fig. 5. An approximative previous approach is shown for comparison. Our new approach agrees very well with a finite-difference estimation from instantons at different temperatures.

Using the results in Fig. 4 and Fig. 5 and the classical expressions for Q_{t-r} we obtain the thermal rate constants depicted in Fig. 6. One can see clearly a very good agreement between the new approach and the conventional determinant method. The highest deviations

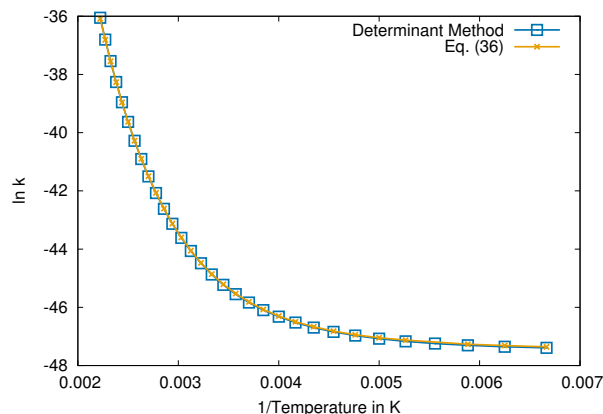


Figure 6: Rate constants in atomic units for the reaction of methylhydroxycarbene to acetaldehyde. The orange line was calculated using Eq. (15) and the quantities determined in Fig. 4. The blue line was calculated with the conventional determinant method.

between the methods appear at low temperature with the rate constant determined by the new approach being 4.3% larger than the one calculated via the determinant method.

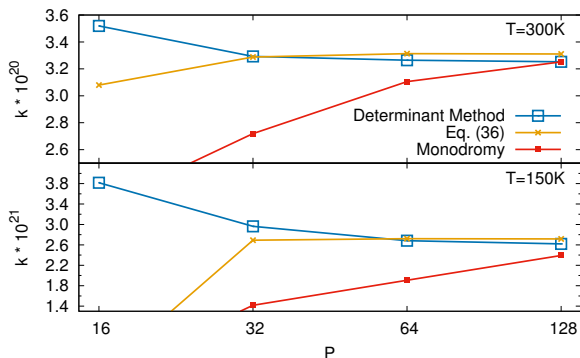


Figure 7: Convergence of the rate constants with the number of images P for two temperatures and for the reaction of methylhydroxycarbene to acetaldehyde. The orange line was calculated using Eq. (15) and the quantities determined in Fig. 4. The blue line was calculated with the conventional determinant method. The red line was obtained from integrating Eq. (30) with $dE/d\beta$ from Eq. (43).

The convergence of both methods with P is displayed in Fig. 7 for two temperatures, $T = 300$ K (top) and $T = 150$ K (bottom) and compared to the standard approach of calculating the stability parameters u_i from the monodromy matrix obtained by integrating Eq. (30).⁴² For very few images, all three methods are inaccurate, but the determinant

method is slightly more stable than our new approach. An instanton path with merely 16 images at a temperature so much below T_c results in a rather badly discretized path. At higher numbers of images, it is notable that the new method converges faster to the final result than the determinant method. The integration of Eq. (30) is found to converge slowest with P . This is a trend we have observed in general. It is most clearly visible at $T = 150$ K. Note the different scale of the vertical axes for the two graphs. A higher number of images is computationally easier accessible with the new method, because its computational effort scales lower with the number of images.

Conclusion

When we compare the results of our new algorithm with the determinant method we obtain practically the same rate constants, for the analytical as well as the DFT potential, yet the computational effort for the rate constant calculation is reduced as no matrix diagonalization is required. Instead of diagonalizing a $PD \times PD$ matrix one has to solve two different linear systems of equations. For the calculation of $\frac{dE}{d\beta}$ one has to solve the system in Eq. (45), which requires Hessians as well as gradients at each point of the trajectory. Gradients are not required in the determinant method. However, they are required for the instanton optimization, so no additional effort is needed. The calculation of the fluctuation factor of the instanton is done by solving Eq. (62) for two different right-hand sides. Furthermore the proposed method improves on the previously presented approaches⁴² by providing a rigorously derived and numerically stable way of obtaining stability parameters in multidimensional systems. These are important in the context of microcanonical and canonical instanton theory. While the fundamental bottleneck of any reaction rate constant calculation remains the calculation of energies and Hessians, the new approach might be particularly helpful if one is interested in obtaining thermal rate constants at very low temperature for a system for which a fitted analytic PES is available and therefore a high number of images can be

computed. In these cases the rate constant calculation can be significantly speeded up.

Acknowledgments

The authors thank Dr. J. Meisner for performing the DFT calculations. This work was financially supported by the European Union's Horizon 2020 research and innovation programme (grant agreement No. 646717, TUNNELCHEM). A.L. is financially supported by the Carl-Zeiss Foundation.

Appendix

Analytic Calculation of Q_{RS}

The trajectory of D uncoupled harmonic oscillators in imaginary time is given by

$$\mathbf{X}(\tau) = \frac{x_i'' \sinh(\omega_i \tau) - x_i'' \sinh((\tau - \beta)\omega_i)}{\sinh(\beta\omega_i)} \hat{\mathbf{e}}_i \quad (67)$$

for $i \in [1, \dots, D]$. The corresponding Euclidean action is

$$\mathcal{S}_E(\mathbf{x}', \mathbf{x}'', \beta) = \int_0^{\beta\hbar} \left(\frac{1}{2} \dot{\mathbf{X}}^2 + \frac{1}{2} \sum_i^D \omega_i^2 x_i^2(\tau) \right) d\tau \quad (68)$$

$$= \sum_{i=1}^D \frac{(x_i'^2 + x_i''^2) \cosh(\omega_i \beta) - 2x_i'' x_i'}{\sinh(\omega_i \beta)}. \quad (69)$$

The evaluation of the second derivatives of \mathcal{S}_E evaluated at the point $\mathbf{x}'' = \mathbf{x}' = \mathbf{x}$ yields

$$\left. \frac{\partial^2 \mathcal{S}_E}{\partial \mathbf{x}'_i \partial \mathbf{x}''_j} \right|_{\mathbf{x}'=\mathbf{x}''} = -\frac{\omega_i}{\sinh(\omega_i \beta)} \delta_{i,j} \quad (70)$$

$$\left. \frac{\partial^2 \mathcal{S}_E}{\partial \mathbf{x}'_i \partial \mathbf{x}''_j} \right|_{\mathbf{x}'=\mathbf{x}''} = \omega_i \coth(\omega_i \beta) \delta_{i,j} \quad (71)$$

$$\left. \frac{\partial^2 \mathcal{S}_E}{\partial \mathbf{x}'_i \partial \mathbf{x}''_j} \right|_{\mathbf{x}'=\mathbf{x}''} = \omega_i \coth(\omega_i \beta) \delta_{i,j}. \quad (72)$$

Using Eq. (28) then yields

$$F = \sqrt{\frac{|-\mathbf{b}|}{|\mathbf{a} + 2\mathbf{b} + \mathbf{c}|}} = \sqrt{\frac{(-1)^D}{|\mathbf{M} - \mathbf{1}|}} \quad (73)$$

$$= \prod_{i=1}^D \frac{1}{2 \sinh(\frac{\omega_i}{2} \beta)} \quad (74)$$

which gives for the Q_{RS}

$$Q_{\text{RS}} = \prod_{i=1}^D \frac{1}{2 \sinh(\frac{\omega_i}{2} \beta)} e^{-\beta V(\mathbf{x}_{\text{RS}})}, \quad (75)$$

i.e. the analytic solution of the partition function of a multidimensional harmonic oscillator.

References

- (1) Miyazaki, T., Ed. *Atom Tunneling Phenomena in Physics, Chemistry and Biology*; Springer, Berlin, Germany, 2004.
- (2) Kohen, A., Limbach, H.-H., Eds. *Isotope Effects in Chemistry and Biology*; CRC Press, Boca Raton, FL, USA, 2005.
- (3) Allemann, R. K., Scrutton, N. S., Eds. *Quantum Tunnelling in Enzyme-Catalysed Reactions*; RSC Publishing, Cambridge, UK, 2009.
- (4) Kohen, A. Kinetic Isotope Effects as Probes for Hydrogen Tunneling, Coupled Motion and Dynamics Contributions to Enzyme Catalysis. *Prog. React. Kinet. Mech.* **2003**, *28*, 119–156.
- (5) Nagel, Z. D.; Klinman, J. P. Tunneling and Dynamics in Enzymatic Hydride Transfer. *Chem. Rev.* **2006**, *106*, 3095–3118.
- (6) Borden, W. T. Reactions that involve tunneling by carbon and the role that calculations have played in their study. *WIREs Comput. Mol. Sci.* **2016**, *6*, 20–46.

- (7) Meisner, J.; Kästner, J. Atom-Tunneling in Chemistry. *Angew. Chem. Int. Ed.* **2016**, *55*, 5400–5413.
- (8) Fernández-Ramos, A.; Miller, J. A.; Klippenstein, S. J.; Truhlar, D. G. Modeling the Kinetics of Bimolecular Reactions. *Chem. Rev.* **2006**, *106*, 4518–4584.
- (9) Pu, J.; Gao, J.; Truhlar, D. G. Multidimensional Tunneling, Recrossing, and the Transmission Coefficient for Enzymatic Reactions. *Chem. Rev.* **2006**, *106*, 3140–3169.
- (10) Nyman, G. Computational methods of quantum reaction dynamics. *Int. J. Quant. Chem.* **2014**, *114*, 1183–1198.
- (11) Kästner, J. Theory and Simulation of Atom Tunneling in Chemical Reactions. *WIREs Comput. Mol. Sci.* **2014**, *4*, 158–168.
- (12) Langer, J. S. Theory of the condensation point. *Ann. Phys. (N.Y.)* **1967**, *41*, 108–157.
- (13) Langer, J. S. Statistical theory of the decay of metastable states. *Ann. Phys. (N.Y.)* **1969**, *54*, 258–275.
- (14) Miller, W. H. Semiclassical limit of quantum mechanical transition state theory for nonseparable systems. *J. Chem. Phys.* **1975**, *62*, 1899–1906.
- (15) Coleman, S. Fate of the false vacuum: Semiclassical theory. *Phys. Rev. D* **1977**, *15*, 2929–2936.
- (16) Callan Jr., C. G.; Coleman, S. Fate of the false vacuum. II. First quantum corrections. *Phys. Rev. D* **1977**, *16*, 1762–1768.
- (17) Affleck, I. Quantum-Statistical Metastability. *Phys. Rev. Lett.* **1981**, *46*, 388–391.
- (18) Benderskii, V. A.; Makarov, D. E.; Wight, C. A. One-Dimensional Models. *Adv. Chem. Phys.* **1994**, *88*, 55–95.

- (19) Feynman, R. P.; Hibbs, A. R. *Quantum Mechanics and Path Integrals*; McGraw-Hill, 1965.
- (20) Arnaldsson, A. Calculation of quantum mechanical rate constants directly from ab initio atomic forces. Ph.D. thesis, University of Washington, 2007.
- (21) Andersson, S.; Nyman, G.; Arnaldsson, A.; Manthe, U.; Jónsson, H. Comparison of Quantum Dynamics and Quantum Transition State Theory Estimates of the H + CH₄ Reaction Rate. *J. Phys. Chem. A* **2009**, *113*, 4468–4478.
- (22) Rommel, J. B.; Goumans, T. P. M.; Kästner, J. Locating instantons in many degrees of freedom. *J. Chem. Theory Comput.* **2011**, *7*, 690–698.
- (23) Rommel, J. B.; Kästner, J. Adaptive Integration Grids in Instanton Theory Improve the Numerical Accuracy at Low Temperature. *J. Chem. Phys.* **2011**, *134*, 184107.
- (24) Faddeev, L.; Popov, V. Feynman diagrams for the Yang–Mills field. *Phys. Lett. B* **1967**, *25*, 29–30.
- (25) Kleinert, H. *Path Integrals in Quantum Mechanics, Statistics, Polymer Physics, and Financial Markets*, 5th ed.; World Scientific, 2009.
- (26) Coleman, S. Quantum Tunneling and negative Eigenvalues. *Nucl. Phys. B* **1988**, *298*, 178–186.
- (27) Hänggi, P.; Talkner, P.; Borkovec, M. Reaction-rate theory: fifty years after Kramers. *Rev. Mod. Phys.* **1990**, *62*, 251–341.
- (28) Messina, M.; Schenter, G. K.; Garrett, B. C. A variational centroid density procedure for the calculation of transmission coefficients for asymmetric barriers at low temperature. *J. Chem. Phys.* **1995**, *103*, 3430.

- (29) Richardson, J. O.; Althorpe, S. C. Ring-polymer molecular dynamics rate-theory in the deep-tunneling regime: Connection with semiclassical instanton theory. *J. Chem. Phys.* **2009**, *131*, 214106.
- (30) Kryvohuz, M. Semiclassical instanton approach to calculation of reaction rate constants in multidimensional chemical systems. *J. Chem. Phys.* **2011**, *134*, 114103.
- (31) Althorpe, S. C. On the equivalence of two commonly used forms of semiclassical instanton theory. *J. Chem. Phys.* **2011**, *134*, 114104.
- (32) Richardson, J. O. Ring-polymer instanton theory. *J. Chem. Phys.* **2018**, *148*, 200901.
- (33) Richardson, J. O. Derivation of instanton rate theory from first principles. *J. Chem. Phys.* **2016**, *144*, 114106.
- (34) Richardson, J. O. Microcanonical and thermal instanton rate theory for chemical reactions at all temperatures. *Faraday Disc.* **2016**, *195*, 49–67.
- (35) Richardson, J. O. Ring-polymer instanton theory. *Int. Rev. Phys. Chem.* **2018**, *37*, 171–216.
- (36) Seideman, T.; Miller, W. H. Calculation of the cumulative reaction probability via a discrete variable representation with absorbing boundary conditions. *J. Chem. Phys.* **1992**, *96*, 4412–4422.
- (37) Miller, W. H. Direct and correct Calculation of Canonical and Microcanonical Rate Constants for Chemical Reactions. *J. Phys. Chem. A* **1998**, *102*, 793–806.
- (38) Miller, W. H. Spiers Memorial Lecture Quantum and semiclassical theory of chemical reaction rates. *Faraday Discuss.* **1998**, *110*, 1–21.
- (39) Takayanagi, K. On the Inelastic Collision between Molecules, II: Rotational Transition of H₂-molecule in the Collision with another H₂-molecule. *Prog. Theor. Phys.* **1952**, *8*, 497–508.

- (40) Bowman, J. M. Reduced dimensionality theory of quantum reactive scattering. *J. Phys. Chem.* **1991**, *95*, 4960–4968.
- (41) Kryvohuz, M. On the derivation of semiclassical expressions for quantum reaction rate constants in multidimensional systems. *J. Chem. Phys.* **2013**, *138*, 244114.
- (42) McConnell, S. R.; Löhle, A.; Kästner, J. Rate constants from instanton theory via a microcanonical approach. *J. Chem. Phys.* **2017**, *146*, 074105.
- (43) Gutzwiller, M. C. Periodic Orbits and Classical Quantization Conditions. *J. Math. Phys.* **1971**, *12*, 343–358.
- (44) Gutzwiller, M. C. Phase Integral Approximation in Momentum Space and the Bound States of an Atom. *J. Math. Phys.* **1967**, *8*, 1979–2000.
- (45) Richardson, J. O.; Bauer, R.; Thoss, M. Semiclassical Green’s functions and an instanton formulation of electron-transfer rates in the nonadiabatic limit. *J. Chem. Phys.* **2015**, *143*, 134115.
- (46) Richardson, J. O. Ring-polymer instanton theory of electron transfer in the nonadiabatic limit. *J. Chem. Phys.* **2015**, *143*, 134116.
- (47) Müller, K.; Brown, L. D. Location of saddle points and minimum energy paths by a constrained simplex optimization procedure. *Theor. Chim. Acta* **1979**, *53*, 75–93.
- (48) McConnell, S. R.; Kästner, J. Instanton rate constant calculations close to and above the crossover temperature. *J. Comput. Chem.* **2017**, *38*, 2570–2580.
- (49) Schreiner, P. R.; Reisenauer, H. P.; Ley, D.; Gerbig, D.; Wu, C.-H.; Allen, W. D. Methylhydroxycarbene: Tunneling Control of a Chemical Reaction. *Science* **2011**, *332*, 1300–1303.
- (50) Kästner, J. The Path Length Determines the Tunneling Decay of Substituted Carbenes. *Chem. Eur. J.* **2013**, *19*, 8207–8212.

- (51) Dirac, P. Quantum Mechanics of Many-Electron Systems. *Proc. Royal Soc. (London) A* **1929**, *123*, 714–733.
- (52) Slater, J. A simplification of the Hartree-Fock method. *Phys. Rev.* **1951**, *81*, 385–390.
- (53) Vosko, S. H.; Wilk, L.; Nusair, M. Accurate spin-dependent electron liquid correlation energies for local spin density calculations: a critical analysis. *Can. J. Phys.* **1980**, *58*, 1200–1211.
- (54) Becke, A. D. Density-functional exchange-energy approximation with correct asymptotic behavior. *Phys. Rev. A* **1988**, *38*, 3098–3100.
- (55) Lee, C.; Yang, W.; Parr, R. G. Development of the Colle-Salvetti correlation-energy formula into a functional of the electron density. *Phys. Rev. B* **1988**, *37*, 785–789.
- (56) Becke, A. D. Density-functional thermochemistry. III. The role of exact exchange. *J. Chem. Phys.* **1993**, *98*, 5648.
- (57) Weigend, F.; Ahlrichs, R. Balanced basis sets of split valence, triple zeta valence and quadruple zeta valence quality for H to Rn: Design and assessment of accuracy. *Phys. Chem. Chem. Phys.* **2005**, *7*, 3297–3305.
- (58) TURBOMOLE, a development of University of Karlsruhe and Forschungszentrum Karlsruhe GmbH, 1989-2007, TURBOMOLE GmbH, since 2007; available from <http://www.turbomole.com>.
- (59) Kästner, J.; Carr, J. M.; Keal, T. W.; Thiel, W.; Wander, A.; Sherwood, P. DL-FIND: an Open-Source Geometry Optimizer for Atomistic Simulations. *J. Phys. Chem. A* **2009**, *113*, 11856–11865.
- (60) Metz, S.; Kästner, J.; Sokol, A. A.; Keal, T. W.; Sherwood, P. ChemShell—a modular software package for QM/MM simulations. *WIREs Comput. Mol. Sci.* **2014**, *4*, 101–110.

- (61) Eichkorn, K.; Weigend, F.; Treutler, O.; Ahlrichs, R. Auxiliary basis sets for main row atoms and transition metals and their use to approximate Coulomb potentials. *Theor. Chem. Acc.* **1997**, *97*, 119–124.